PHYSICAL CHEMISTRY

Direct Observation of the Three-Dimensional Velocity Distributions of Cl($^2P_{3/2,1/2}$) Atoms in the Photodissociation of Selected Chlorides

A. I. Chichinin[a], T. Einfeld[b], C. Maul[b], and K.-H. Gericke[b]

Presented by Academician Yu.D. Tsvetkov May 12, 2005
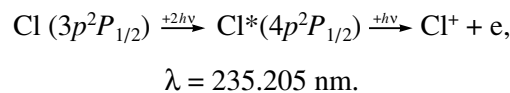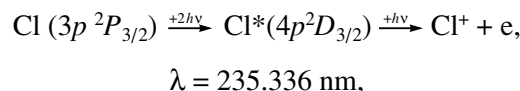
Received May 26, 2005

The recent breakthrough in the study of molecular dynamics is due to the advent of a technique for imaging the spatial distributions of photodissociation or chemical reaction products [1] and, especially, of an improved version of this method referred to as velocity map imaging (1997) [2]. In this technique, the products are ionized by means of resonance-enhanced multiphoton ionization (REMPI) and the nascent ions are accelerated by an electric field and detected as scintillations on a phosphorescent screen. Recently, we suggested a new version of the imaging technique [3], an alternative to velocity map imaging. The major difference between this method and the imaging technique is that the phosphorescent screen is exchanged for a position-sensitive delay-line detector (DLD) [4] with high time resolution. The DLD is a ceramic frame on which two wires are wound parallel to the X and Y axes, which are delay lines. A charge appearing somewhere on the delay line is propagated in both directions toward the line ends, where the signal arrival time is recorded. Each ion gives rise to two pairs of times (X_1, X_2) and (Y_1, Y_2) for the delay lines along the X and Y axes, respectively. The coordinates X and Y of this event in time units can be calculated as $(X_1 - X_2, Y_1 - Y_2)$, and the time of the event, which is the Z coordinate, can be calculated as $\frac{1}{4}(X_1 + X_2 + Y_1 + Y_2)$. Thus, the DLD gives three coordinates of the event from the four times measured. The transverse velocities v_x and v_y are determined from the X and Y coordinates of the collision of ions with the surface of

the detector, and the longitudinal velocity v_z is calculated from the time of collision. This method allows one to measure v_x, v_y, and v_z, whereas the velocity map imaging technique gives only v_x and v_y. As a result, new information becomes available, in particular, anisotropy parameters $\beta(v)$ that are a function of velocity. The knowledge of $\beta(v)$ turns out to be very useful, especially for analysis of complicated systems. In this work, we selected complicated chloride systems, such as $COCl_2$, $CSCl_2$, S_2Cl_2, and $SOCl_2$.

The setup was described in [3]. It consists of a time-of-flight mass spectrometer. In its center, a continuous supersonic molecular beam (along the Y axis) and a laser beam (along the X axis) intersect. The mass spectrometer is a high-vacuum chamber with a homogeneous electric field (along the Z axis), which accelerates the positive photoions created by means of REMPI in the direction toward the DLD. The chamber meets collisionless conditions. A dye laser, which was pumped with a Nd:YAG laser, was used. The dye laser fundamental was first doubled with the use of a BBO crystal and then focused by a lens ($f = 20$ cm) into the mass spectrometer chamber. The same radiation was used for both the photodissociation of chlorides and the detection of chlorine atoms. The laser energy was low enough to detect on average one ion per ten laser pulses. Cl($^2P_{3/2}$) and Cl($^2P_{1/2}$) atoms were detected by REMPI according to the schemes [5]

$$Cl\,(3p\ ^2P_{3/2}) \xrightarrow{+2h\nu} Cl^*(4p\,^2D_{3/2}) \xrightarrow{+h\nu} Cl^+ + e,$$

$$\lambda = 235.336 \text{ nm},$$

$$Cl\,(3p^2P_{1/2}) \xrightarrow{+2h\nu} Cl^*(4p\,^2P_{1/2}) \xrightarrow{+h\nu} Cl^+ + e,$$

$$\lambda = 235.205 \text{ nm}.$$

These schemes involve resonant two-photon excitation followed by nonresonant single-photon ionization.

[a] Institute of Chemical Kinetics and Combustion,
   Siberian Division, Russian Academy of Sciences,
   Institutskaya ul. 3, Novosibirsk, 630090 Russia
[b] Institut für Physikalische und Theoretische Chemie,
   Technische Universität Braunschweig,
   Hans-Sommer-Str. 10, D-38106 Braunschweig,
   Germany

The standard expression for the angular distribution of photoproducts

$$I(\theta) \simeq \sin\theta\left[1 + \frac{\beta}{2}(3\cos^2\theta - 1)\right] \quad (-1 \le \beta \le 2),$$
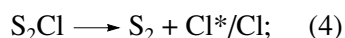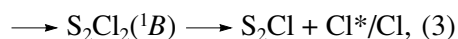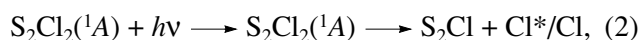
was used for fitting the experimental data. Here, θ is the polar spherical angle measured from the direction of the electric field of the laser radiation. The anisotropy parameter β can be calculated in the limit of instantaneous dissociation [6, 7] as

$$\beta = 3\cos^2\chi - 1, \quad (1)$$

where χ is the angle between the transition dipole moment (μ) and the escape velocity of a photofragment.

The quantitative results of analysis are presented in the table. The velocity distributions ($W(v)$ (or energy distributions $W(E_t)$)) of chlorine atoms, as well as the $\beta(v)$ plots, are shown in Figs. 1–4. For the sake of illustration, we report on the analysis of photodissociation dynamics for S_2Cl_2 and mention briefly such results for the other three chlorides.

1. The ground state of the S_2Cl_2 molecule (=Cl–S–S–Cl, symmetry C_2) has symmetry ^1A. Upon the absorption of a photon, the following processes are energetically possible:

$$S_2Cl_2(^1A) + h\nu \longrightarrow S_2Cl_2(^1A) \longrightarrow S_2Cl + Cl^*/Cl, \quad (2)$$
$$\longrightarrow S_2Cl_2(^1B) \longrightarrow S_2Cl + Cl^*/Cl, \quad (3)$$
$$S_2Cl \longrightarrow S_2 + Cl^*/Cl; \quad (4)$$

the existence of the excited state ^1A has been documented, while the existence of the ^1B state is only conjectured [9]. The latter should be higher in energy than the ^1A state. Channel (2) corresponds to the optical transition $^1A \longrightarrow {}^1A$; hence, $\mu \parallel C_2$ (here, C_2 is the symmetry axis). In this case, χ is the angle between the symmetry axis and the S–Cl bond. Using formula (1), we find that $\beta_2 = 0.48$. Channel (3) corresponds to the optical transition $^1A \longrightarrow {}^1B$; hence, $\mu \perp C_2$ and, according to formula (1), $-0.71 \le \beta_3 \le 0.37$. As is known, the 193-nm photolysis of S_2Cl_2 yields chlorine atoms with an anisotropy parameter of –0.3 [9]. Therefore, it is natural to assume $\beta_3 \le -0.3$ for channel (3). The β parameter for channel (4) is difficult to predict; however, it is evident that, when the first chlorine atom is removed from the molecule, the S_2Cl fragment considerably changes its orientation in space. It is reasonable to expect that the angular distribution for this channel is isotropic; therefore, $\beta_4 = 0$. Figure 1 shows that, for "fast" $Cl(^2P_{3/2})$ and $Cl(^2P_{1/2})$ atoms, the anisotropy parameter is 0.45 and 0.24, respectively. This means that the $Cl(^2P_{3/2})$ atoms are formed in process (2), while the $Cl(^2P_{1/2})$ atoms are mainly formed in process (2) but some fraction of them are also formed in (3). For "slow" and "intermediate" chlorine atoms, $\beta \approx 0$ and

Results of studying the photodissociation of chlorides

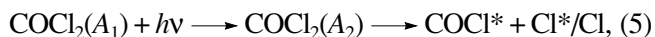| Chloride (σ_{235}, cm^2)	Dissociation channel[a]	P[b], %	β	E_{max}^c, kJ/mol
S_2Cl_2 (6×10^{-18})	(2)	11.2	0.45 ± 0.12	123.0
	(3)	27.4	-0.25 ± 0.07	53.6
	(4)	26.4	0 ± 0.05	16.8
	(2)*	13.2	0.24 ± 0.12[d]	124.9[d]
	(3)*	6.3	0.24 ± 0.12[d]	124.9[d]
	(3)*	7.8	-0.25 ± 0.07	51.2
	(4)*	7.7	0 ± 0.05	18.6
$COCl_2$ (9×10^{-20})	(6)	47	0	10
	(5)	31	0.7 ± 0.1	36
	(6)*	3	0	6.6
	(5)*	19	0.6 ± 0.1	45
$SOCl_2$ (7×10^{-18})	(7)	28.3	0.85 ± 0.08	113.0
	(8)	17.2	0.10 ± 0.13	57.4
	(9)	19.5[e]	0.10 ± 0.12	20.2
	(10)	19.5[e]	0.00 ± 0.07	11.2
	(7)*	19.2	0.68 ± 0.07	113
	(8)*	12.6	0.10 ± 0.13	57
	(9)*	3.2[e]	0.10 ± 0.12	20
	(10)*	3.2[e]	0.00 ± 0.06	11
$SCCl_2$ (4×10^{-18})	(11)	2	0.2 ± 0.07	116.6
	(12)	32	0.03 ± 0.05	47.4
	(13)	19	-0.07 ± 0.06	12.5
	(11)*	3.5	0.08 ± 0.07	121.5
	(12)*	33.5	0.03 ± 0.06	54.2
	(13)*	10	0.15 ± 0.08	21.5

Note: [a] Channels leading to $Cl(^2P_{1/2})$ are asterisked, and those leading to $Cl(^2P_{3/2})$ are unlabeled; [b] the probability of a given channel; [c] the position of the maximum for a given channel; [d] parameters for the peak corresponding to a combination of channels (2)* and (3)*; [e] the overall probability for channels (9) and (10).

$\beta \approx -0.25$, respectively. Hence, these velocity ranges correspond to channels (3) and (4), respectively. The decomposition of the $W(v)$ distributions into three components is shown in Fig. 1, and the results of this decomposition are presented in the table.
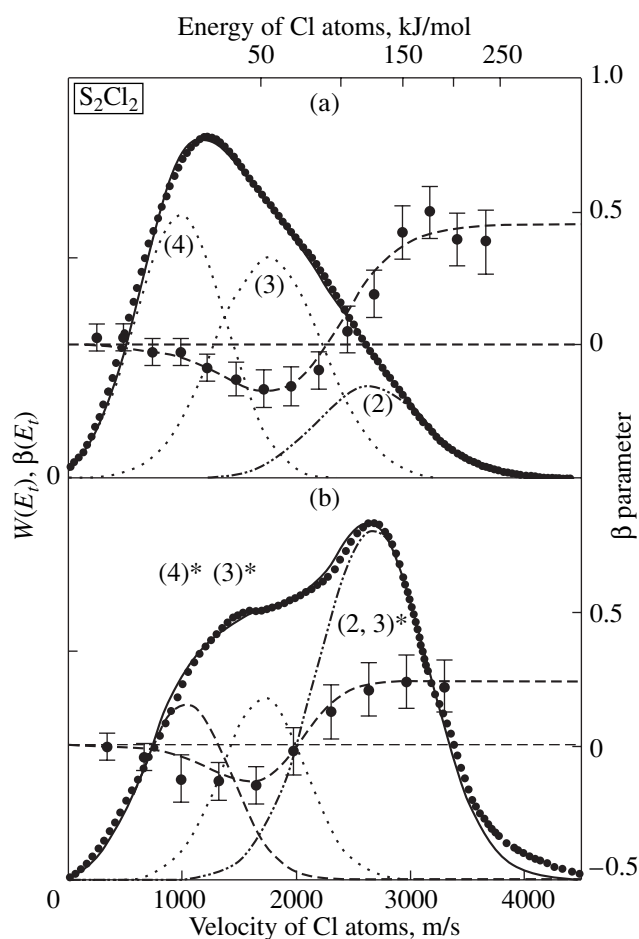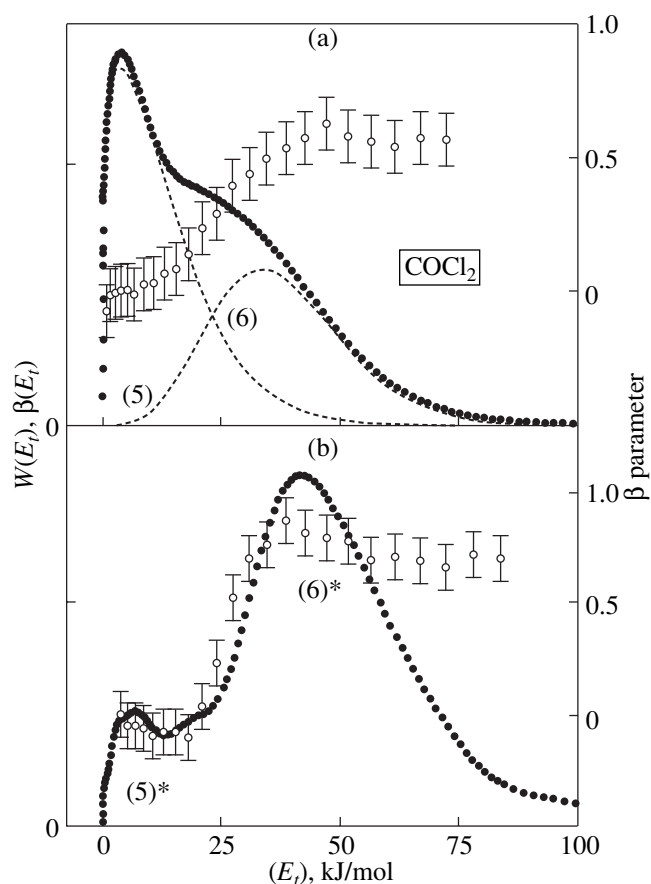
Fig. 1. Photolysis of S_2Cl_2: (a) $Cl(^2P_{3/2})$ and (b) $Cl^*(^2P_{1/2})$. The $W(v)$ curves show the velocity distributions of chlorine atoms. Here and in Figs. 2–4, data points are the corresponding β parameters (right-hand scale). Dashed lines show the decomposition of the velocity distribution into three components.

Fig. 2. Photolysis of $COCl_2$: (a) $Cl(^2P_{3/2})$ and (b) $Cl^*(^2P_{1/2})$. The $W(E_t)$ curves show the kinetic energy distributions of chlorine atoms. Dashed lines show the decomposition of the kinetic energy distribution into two components.

2. The photodissociation dynamics of the $COCl_2$ molecule (symmetry C_{2v}) is somewhat simpler. The absorption of a photon entails the dissociation into the three particles [10]
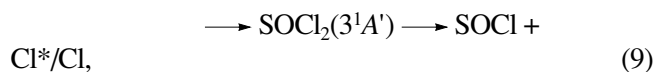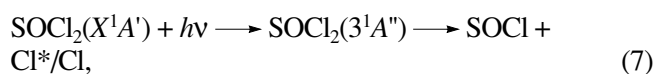
$$COCl_2(A_1) + h\nu \longrightarrow COCl_2(A_2) \longrightarrow COCl^* + Cl^*/Cl, \quad (5)$$

$$COCl^* \longrightarrow CO + Cl^*/Cl. \quad (6)$$

The $W(E_t)$ distributions were decomposed into two components (Fig. 2). The results of this decomposition are listed in the table. From the energies, it is evident that fast chlorine atoms are formed in process (5) and slow atoms, in process (6). If the ClCCl angle (ClCCl = $\chi = 111.3°$) is taken as χ and substituted into Eq. (1), we obtain $\beta = 1.04$ for process (5), which somewhat overestimates the experimental values $\beta = 0.6$–0.7. Our calculations show that this discrepancy is explained by the rotation of the $COCl_2$ molecule and that the lifetime of

the excited $COCl_2^*$ molecule is ≈230 fs. For channel (6), the angular distribution of the photoproducts is virtually isotropic, which is due to the longer (as compared to the rotation period) lifetime of the $COCl^*$ fragment.

3. The excited states of the $SOCl_2$ molecule were studied with the use of quantum-chemical calculations. It turned out that only two excited states of the $SOCl_2$ molecule and one excitation state of the $SOCl$ fragment should be taken into account:

$$SOCl_2(X^1A') + h\nu \longrightarrow SOCl_2(3^1A'') \longrightarrow SOCl + Cl^*/Cl, \quad (7)$$

$$\longrightarrow SOCl_2(3^1A') \longrightarrow SOCl^* + Cl^*/Cl, (8)$$

$$\longrightarrow SOCl_2(3^1A') \longrightarrow SOCl + Cl^*/Cl, \quad (9)$$

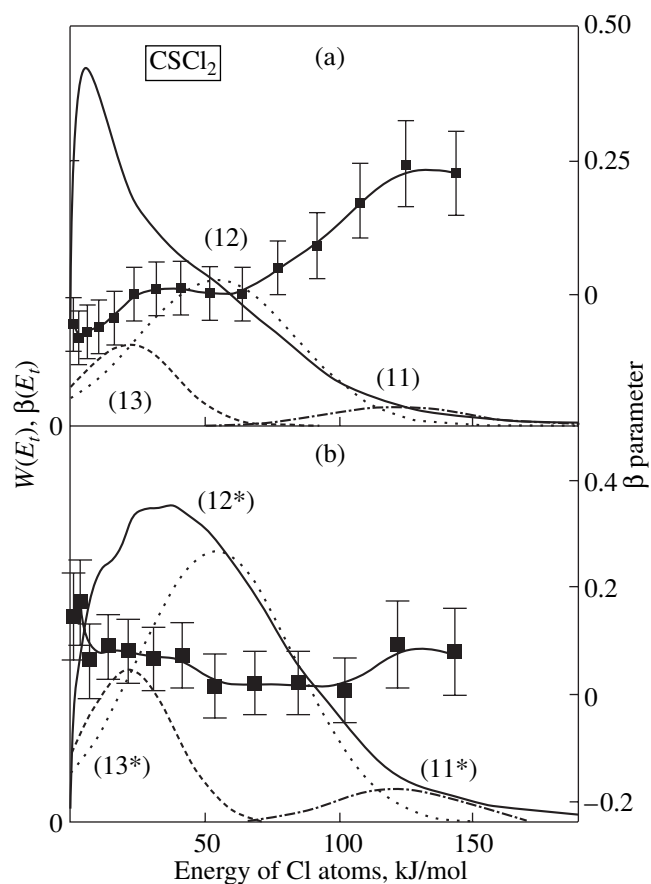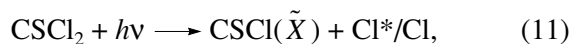$$SOCl \longrightarrow SO + Cl^*/Cl. \quad (10)$$

The existence of four components in the $W(v)$ distributions follows from general considerations and previous experiments. For example, the existence of chan-
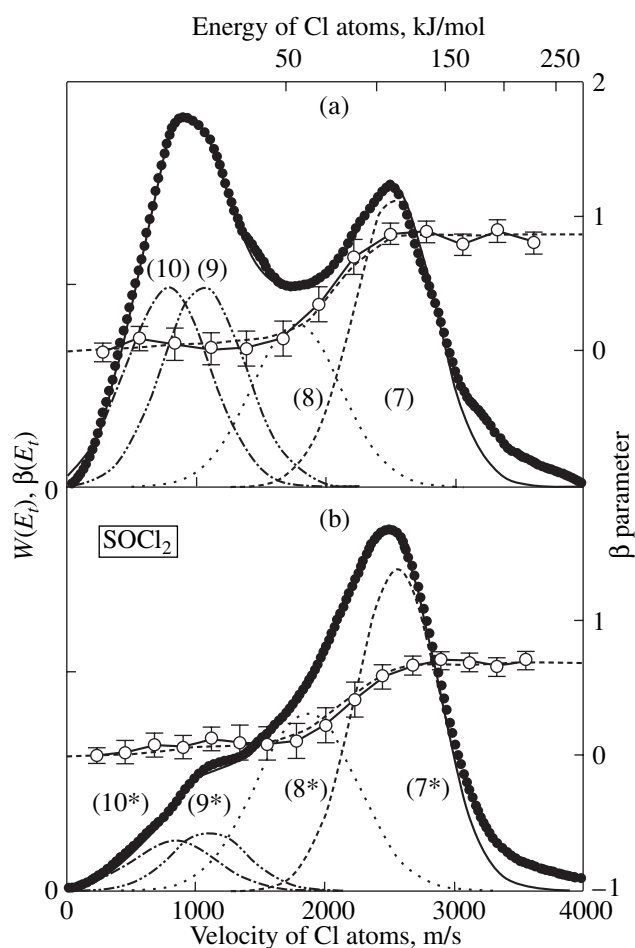
Fig. 3. Photolysis of $SOCl_2$: (a) $Cl(^2P_{3/2})$ and (b) $Cl*(^2P_{1/2})$. The $W(v)$ curves show the velocity distributions of chlorine atoms. Dashed lines show the decomposition of the velocity distribution into four components.

Fig. 4. Photolysis of $CSCl_2$: (a) $Cl(^2P_{3/2})$ and (b) $Cl*(^2P_{1/2})$. The $W(E_t)$ curves show the kinetic energy distributions of chlorine atoms. Dashed lines show the decomposition of the kinetic energy distribution into three components.

nel (10) follows from the observation of vibrationally and translationally cold SO radicals in [11]. Fast chlorine atoms are generated by the optical transition $(A' \longrightarrow A'')$, for which the calculated and experimental β parameters are virtually the same and equal to ≈0.8. The $(A' \longrightarrow A')$ transition gives $β ≈ 0.2$; for channel (10), we assume $β ≈ 0$. Although the decomposition of $W(v)$ into the four components is shown in Fig. 3, it is evident that the two low-velocity components cannot be unambiguously resolved.

4. Finally, the $CSCl_2$ molecule is a simple case in which only dissociation into two particles is possible. The nascent CSCl radical can be in different electronic states ($E(\tilde{X}) = 0$, $E(\tilde{A}) = 77$, and $E(\tilde{B}) = 178$ kJ/mol [12]):

$$CSCl_2 + h\nu \longrightarrow CSCl(\tilde{X}) + Cl*/Cl, \qquad (11)$$

$$\longrightarrow CSCl(\tilde{A}) + Cl*/Cl, \qquad (12)$$

$$\longrightarrow CSCl(\tilde{B}) + Cl*/Cl. \qquad (13)$$

All these channels are observed experimentally (Fig. 4). The above examples show that

(1) Our technique makes it possible to analyze complicated photodissociation dynamics, the $β(v)$ dependences being very useful.

(2) This analysis provides information on the symmetry and energy of the molecular excited states.

(3) The $Cl(^2P_{3/2})$ and $Cl(^2P_{1/2})$ atoms have very different dynamics, which calls for further study.

REFERENCES

1. Chandler, D.W. and Houston, P.L., *J. Chem. Phys.*, 1987, vol. 87, no. 2, pp. 1445–1447.

2. Eppink, A.T.J.B. and Parker, D.H., *Rev. Sci. Instrum.*, 1997, vol. 68, no. 9, pp. 3477–3484.

3. Chichinin, A.I., Einfeld, T., Maul, C., and Gericke, K.-H., *Dokl. Akad. Nauk*, 2005, vol. 402, no. 5, pp. 633–638

[*Dokl. Phys. Chem.* (Engl. Transl.), vol. 402, part 2, pp. 96–100].

4. Jagutzki, O., Mergel, V., Ullmann-Pfleger, K.U., et al., *Nucl. Instrum. Methods Phys. Res. A*, 2002, vol. 477, no. 113, pp. 244–249.

5. Arepalli, S., Presser, N., Robie, D., and Gordon, R.J., *Chem. Phys. Lett.*, 1985, vol. 118, no. 1, pp. 88–92.

6. Zare, R.N., *Mol. Photochem.*, 1972, vol. 4, p. 1.

7. Busch, G.E. and Wilson, K.R., *J. Chem. Phys.*, 1972, vol. 56, no. 7, pp. 3638–3654.

8. Lindner, J., Niemann, R., and Tiemann, E., *J. Mol. Spectrosc.*, 1994, vol. 165, no. 2, pp. 358–367.

9. Lee, Y.R., Chiu, C.L., Tiemann, E., and Lin, S.M., *J. Chem. Phys.*, 1999, vol. 110, no. 14, pp. 6812–6819.

10. Maul, C., Haas, T., and Gericke, K.-H., *J. Phys. Chem. A*, 1997, vol. 101, no. 36, pp. 6619–6632.

11. Roth, M., Maul, C., and Gericke, K.-H., *Phys. Chem. Chem. Phys.*, 2002, vol. 4, no. 13, pp. 2932–2940.

12. Hachey, A., Grein, F., and Steer, R.P., *Can. J. Chem.*, 1993, vol. 71, p. 112.